

## INFLUENCE OF THE SELF-BIAS VOLTAGE ON THE MICRO-STRUCTURE OF HYDROGENATED AMORPHOUS CARBON FILMS ELABORATED BY RF-PECVD

Reçu le 10/11/2007 – Accepté le 26/05/2008

### Résumé

Des couches de carbone amorphe hydrogéné (a-C:H) ont été préparées à la température ambiante par la technique RF-PECVD, en utilisant différentes tensions d'auto-polarisation du substrat (150 V – 240 V). La microstructure de ces couches fut ensuite analysée par deux techniques d'investigation complémentaires : la spectroscopie d'absorption infrarouge et la spectroscopie Raman. Les résultats obtenus grâce à la première technique montrent que l'hydrogène est lié aussi bien aux atomes de carbone en configuration sp<sup>2</sup>C, qu'en configuration sp<sup>3</sup>C, pour tous les échantillons étudiés. Ainsi, plus de 60% de l'hydrogène est lié aux groupes sp<sup>3</sup>CH<sub>x</sub> (x = 2, 3), alors que seulement 13 à 17% de cet élément est lié aux espèces sp<sup>2</sup>CH dans des amas graphitiques (probablement des anneaux aromatiques). L'influence de la polarisation V<sub>b</sub> des substrats sur la microstructure des couches a-C:H est également démontrée par l'analyse Raman que nous avons effectuée. En effet, une relation linéaire existe bien entre le rapport de l'intensité intégrée du pic D et celle du pic G (ID/IG) et la largeur à mi-hauteur du pic G (ΔG), pour des valeurs de V<sub>b</sub> relativement élevées. : lorsque V<sub>b</sub> augmente, ID/IG augmente également alors que ΔG devient faible. Ce qui signifie que la largeur ΔG est fortement affectée par la graphitisation progressive du matériau, et donc la présence d'amas graphitiques. Les valeurs observées pour ΔG (166 à 178 cm<sup>-1</sup>) et le fait que ID/IG soit inférieur à 1, suggèrent que la taille des amas graphitiques ne devrait pas dépasser 10 Å. Ces dernières caractéristiques, ainsi que la largeur du gap optique déterminée par des mesures dans l'UV/visible, et les valeurs relativement faibles de la concentration d'hydrogène – déterminées à partir des spectres d'absorption infrarouge- suggèrent que les couches a-C:H étudiées ont des propriétés microstructurales comprises entre celles des couches polymériques et celles des couches DLC.

**Mots clés:** PECVD, a-C:H, FTIR, spectroscopie Raman, graphitisation

### Abstract

Hydrogenated amorphous carbon films (a-C:H) were deposited at room temperature in an rf-PECVD reactor using different DC self-biases (150 – 240 V). The microstructure of the films was then analysed by infrared transmission spectroscopy and Raman spectroscopy. The IR results show that hydrogen is bonded to both sp<sup>3</sup>C and sp<sup>2</sup>C atoms in all samples: more than 60% of bonded H is in sp<sup>3</sup>CH<sub>x</sub> groups (x = 2, 3) while only 13 to 17% is in sp<sup>2</sup>CH species in graphitic clusters (probably aromatic rings). The influence of self-bias voltage V<sub>b</sub> on the microstructure of the a-C:H films is also demonstrated by Raman scattering analysis. Indeed, a linear relationship between the ratio of the integrated intensity of the D peak over that of the G one (ID/IG) and the G peak FWHM (ΔG) was found for films prepared at relatively high V<sub>b</sub> values (V<sub>b</sub> higher than -150 V). As the DC bias V<sub>b</sub> increases, the ratio ID/IG increases while ΔG becomes narrower. Also ΔG is strongly affected by the graphitization of the material and hence the presence of graphitic clusters. The observed values of ΔG (166 – 178 cm<sup>-1</sup>) and ID/IG (≤ 1) for our films suggest that the graphitic clusters sizes are less than 10 Å. Moreover, the relative low hydrogen content of these films, as shown by infrared transmission spectra, in addition to the former characteristics and to the values of band gap width, indicate that our a-C:H films seem to exhibit properties which lie between those of polymeric and DLC films.

**Keywords:** PECVD, a-C:H, FTIR, Raman spectroscopy, graphitization

N. HADJ-ZOUBIR<sup>1</sup>

F. BOUKHORS<sup>1</sup>

R. BAGHDAD<sup>1</sup>

K. ZELLAMA<sup>2</sup>

<sup>1</sup> Laboratoire de Génie Physique, Université Ibn Khaldoun, B.P. 78, Tiaret 14000, Algérie

<sup>2</sup> Laboratoire de Physique de la Matière Condensée, Faculté des Sciences, 33 Rue Saint-Leu, 80039 Amiens, France

### ملخص

صنعت بطريقة الترسيب الكيمائي، باستخدام (a-C:H) نتناول في هذه المذكرة دراسة مفصلة للتركيبية البنوية لطبقات من الكربون الهيدروجيني اللابلوري V أثناء الترسيب من -150 إلى 240 (Vp) في درجة حرارة مثالية ثابتة مع تغيير قيم فرق الكمون المطبق (PECVD) غاز فحم هيدروجيني بوجود بلازما (RAMAN) لهذا الغرض، نستعين بتقنيتين تجريبيتين متممتين وهما: طيفية أشعة تحت الحمراء و طيفية

إن النتائج المتحصل عليها باستعمال التقنية الأولى، تشير إلى أن الهيدروجين الموجود في الطبقات المدروسة ملتصق بذرات الكربون الموجودة في مجموعات مع sp<sup>3</sup>CH<sub>x</sub> لتكون أصناف (sp<sup>3</sup>C). التحاليل المدققة تبين أن أكثر من 60% من ذرات الهيدروجين ملتصقة بمجموعات (sp<sup>3</sup>C) و (sp<sup>2</sup>C) من نوع هذه الأخيرة هي في الأصل كومات (sp<sup>2</sup>CH) لتكون أصناف من نوع (sp<sup>2</sup>C)، بينما 13 إلى 17% فقط من الهيدروجين ملتصق بمجموعات (sp<sup>2</sup>C) و (sp<sup>3</sup>C) من نوع غرافيتية في شكل حلقات عطرية

، إذ أننا وجدنا علاقة خطية بين نسبة (a-C:H) أثر ملحوظ على التركيبية البنوية لطبقات (Vp) أن لفرق الكمون (RAMAN) من جهة أخرى، تؤكد تقنية و انخفاض قيمة العرض (ID/IG)، نلاحظ ارتفاع النسبة (Vp): عند ارتفاع (G) لذروة (ΔG) و العرض النصف (ID/IG) (G) و (D) شدتي الذروتين و ( التي تميز طبقاتنا و المتروحة بين (ΔG) متأثر من ظهور تدريجي و متزايد للكومات الغرافيتية. إن قيمة (ΔG). هذه النتائج تعني أن (ΔG) النصفية 166، يبين أن قياس الكومات الغرافيتية لا تتجاوز (ID/IG ≤ 1) التي لا تفوق 1 (ID/IG) و قيمة النسبة (cm<sup>-1</sup> 178-)

كل هذه النتائج، و النتائج الأخرى المتحصل عليها عن طريق تقنيات أخرى، كالتقنيات الضوئية في مجال ما فوق البنفسجي و المرئي، زيادة على تقنية قياس بل بينها DLC. و لا طبقات PLC كيمياية الهيدروجين، تشير إلى أن طبقاتنا خصوصيات بنوية لا هي خصوصيات طبقات

**الكلمات المفتاحية:** الترسيب الكيمائي (PECVD)، طيفية أشعة تحت الحمراء، طيفية (RAMAN)، مرحلة التكوين الغرافيتية.

## Introduction

The physical properties of amorphous carbon (a-C) have been the subject of intense experimental and theoretical studies [1, 2]. Amorphous carbon films are presently being used in wide variety of applications including wear-resistant coatings for hard-disk drives and optical components, as well as in semiconductor devices [3]. The introduction of hydrogen into a-C not only passivates the dangling bonds but also promotes  $sp^3$  bonding, causing an enlargement of the band gap. Hydrogenated amorphous carbon with low hydrogen concentration is often called "hard" a-C:H (Diamond-Like a-C:H or DLC) due to its high hardness, and is characterized by a narrow band gap (0.8 – 1.7 eV). This hard a-C:H contains a large amount of  $sp^2$  carbon in addition to  $sp^3$  carbon. a-C:H with a high hydrogen concentration is known as "soft" a-C:H and has higher values of band gap (1.6 – 4 eV). The low hardness of this material is due to the monovalent hydrogen which serves only as a terminating atom on the carbon skeleton network. Most of the excess of hydrogen is bonded in the  $sp^3$  configuration, which allows soft a-C:H to have a high percentage of  $sp^3$  bonding. In contrast, films with a low hydrogen concentration and a high percentage of  $sp^3$  carbon are referred to tetrahedral a-C:H (ta-C:H). ta-C:H films are a class of DLC for which the C-C  $sp^3$  content can be increased whilst keeping a fixed hydrogen concentration. Thus, most films defined in literature as ta-C:H are just DLCs [4]. The optical band gap can reach 2.3 eV [5]. In this work, we have investigated the microstructure of a-C:H films prepared at different substrate polarizations using a combination of complementary experimental techniques such as Fourier transform infrared (FTIR) spectroscopy and Raman spectroscopy. A correlation between the obtained results using the two techniques was then realized. Optical transmission measurements are also carried out to determine the optical gap and therefore, to get more details about the microstructure of the films.

## 2 Experimental details

The a-C:H films were prepared by plasma enhanced chemical vapour deposition (PECVD) of  $CH_4$  gas at low pressure (0.1 Torr) in a dual electron cyclotron resonance (ECR)-radiofrequency (RF) glow discharge system. The plasma was excited by feeding microwave at a constant power (of about 200 W), into 35 sccm of pure methane. Four different series of films labelled I, II, III and IV with thicknesses varying between 1 and 1.4  $\mu$ m were deposited onto intrinsic crystalline silicon (c-Si), with a self-induced bias voltages applied to the substrate equal to -150 V, -180 V, -210 and -240 V, respectively.

The local microstructure (i.e. C-H and C-C bonding) was studied by mean of FTIR spectroscopy in the range 400-4000  $cm^{-1}$  with a resolution of 4  $cm^{-1}$  using a Nicolet 510 spectrometer and Raman spectroscopy using a Dilor Jobin Yvon spectrophotometer with a 514.5 nm line of an

argon ion laser (maximum power of about 1 mW to avoid annealing effects in the sample). The scattered light was analyzed with a resolution of 4  $cm^{-1}$ . Both FTIR and Raman experiments are conducted on c-Si substrates. Optical transmission measurements were carried out using a Varian spectrophotometer in the wavelength range extending from 180 to 2000 nm, in order to estimate the band gap width.

## 3 Results and discussion

In Fig. 1, we compare typical infrared absorption spectra obtained in the as-deposited state for two samples grown at substrate bias voltage  $V_b = -150$  V (series I) and  $V_b = -240$  V (series IV) in the high stretching frequency range (2700–3200  $cm^{-1}$ ). In this figure, the absorption has been corrected for varying thickness.

As expected, the stretching band is more intense for series I than for series IV, suggesting a higher total bonded H content in the former case. The relative proportion of H content was found to be approximately 17% lower for series IV. These data are consistent with the fact that the high values of  $V_b$ , i.e. high impact energies on the film surfaces, lead to the break of C-H bonds during the films growth, and consequently a release of H atoms.

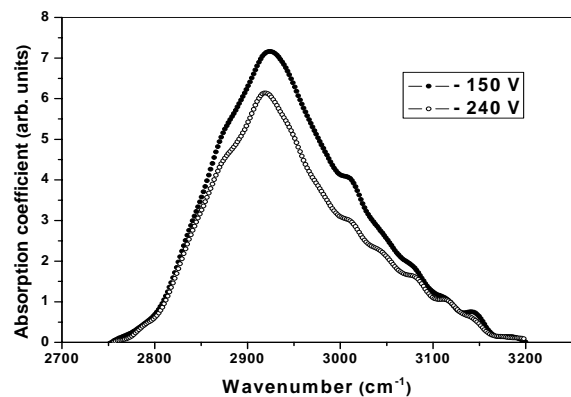


**Figure 1:** Typical FTIR spectra in the stretching modes range obtained for films deposited with  $V_b$  equal to -150 V and -240 V (samples of series I and IV, respectively).

An example of decomposition of the stretching band into a sum of Gaussian contributions corresponding to the different vibration modes is shown in Fig. 2, for samples series I. The assignments of the relevant FTIR peaks of Fig. 2 are reported in Table 1.

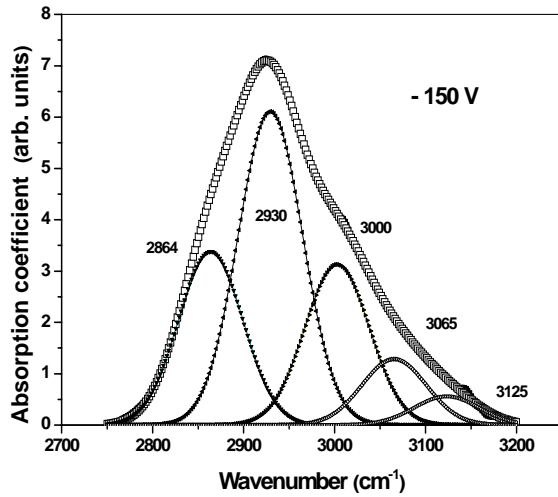


**Figure 2:** Example of decomposition of the stretching band into a sum of Gaussian contributions corresponding to the different vibration modes shown for sample of series I.

Wavenumber (cm-1)	Vibration mode
2864	sp3 CH3 sym
2930	sp3 CH2 asym
3000	sp2 CH olef
3065	sp2 CH2 arom
3125	sp2 CH arom

**Table 1:** Assignments of the a-C:H infrared vibration modes in the 2700 – 3200 cm-1 region.

The data clearly show that H is bonded to both sp<sup>3</sup>C sites, which correspond to wavenumbers below 3000 cm<sup>-1</sup> (in C-H<sub>2</sub> as well as C-H<sub>3</sub> complexes) and to sp<sup>2</sup>C sites, corresponding to wavenumbers in the range 3000-3200 cm<sup>-1</sup> [6]. The proportions of H bonded to sp<sup>3</sup>C and sp<sup>2</sup>C sites can be estimated from the integrated absorption of the stretching components below 3000 cm<sup>-1</sup> and in the 3000-3200 cm<sup>-1</sup> range, respectively. The variation of these proportions with V<sub>b</sub> is presented in Fig. 3.

We note that most of hydrogen is preferentially bonded to sp<sup>3</sup>C sites in a relative proportion of about 65% of the total bonded H content.

The data clearly show that H is bonded to both sp<sup>3</sup>C sites, which correspond to wavenumbers below 3000 cm<sup>-1</sup> (in C-H<sub>2</sub> as well as C-H<sub>3</sub> complexes) and to sp<sup>2</sup>C sites, corresponding to wavenumbers in the range 3000-3200 cm<sup>-1</sup> [6].

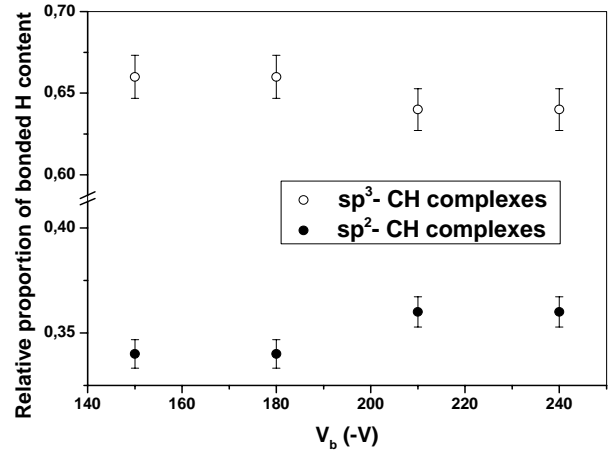


**Figure 3:** Variation of the relative proportion (%) of the H bonded as sp<sup>3</sup>-C-H and sp<sup>2</sup>-C-H complexes, as a function of V<sub>b</sub>

The proportions of H bonded to sp<sup>3</sup>C and sp<sup>2</sup>C sites can be estimated from the integrated absorption of the stretching components below 3000 cm<sup>-1</sup> and in the 3000-3200 cm<sup>-1</sup> range, respectively. The variation of these proportions with V<sub>b</sub> is presented in Fig. 3. We note that most of hydrogen is preferentially bonded to sp<sup>3</sup>C sites in a relative proportion of about 65% of the total bonded H content.

Moreover, Fig. 3 shows that only a slight decrease (66 to 64%) in the proportion of the sp<sup>3</sup>C-H<sub>x</sub> complexes and a slight increase (34 to 36%) in the proportion of the sp<sup>2</sup>C-H<sub>y</sub> groups are observed when increasing V<sub>b</sub>. This suggests that the increase in the self-bias V<sub>b</sub> does not drastically change the microstructure of the films in terms of bonded H to carbon atoms.

In order to get more insight into the analysis of the local microstructure of our films, we considered the changes with V<sub>b</sub> in the IR integrated absorption of the different components that fitted the stretching absorption band, which are located at 2860, 2930, 3000, 3065 and 3120 cm<sup>-1</sup>. The results are presented in Fig. 4.

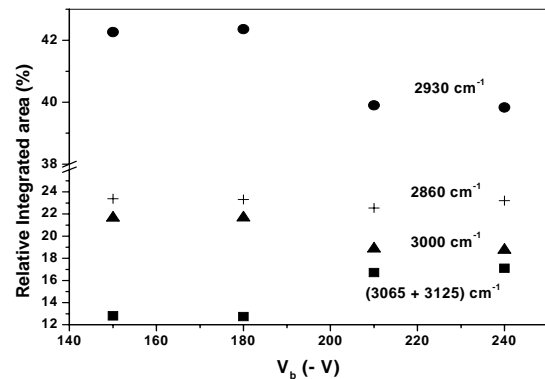


**Figure 4:** Variation of integrated area of the different Gaussian components that fitted the stretching IR absorption band, as a function of V<sub>b</sub>, as indicated.

This figure clearly shows that, as already mentioned above, about 65% of the total bonded H is in sp<sup>3</sup>C-Hx complexes, with, however, a higher proportion of sp<sup>3</sup>C-H<sub>2</sub> complexes (~ 42%). We observe a drastic decrease in this proportion with increasing V<sub>b</sub>, while, in contrast, the proportion of the sp<sup>3</sup>C-H<sub>3</sub> groups stays almost unchanged (about 23%). An important decrease in the proportion of the sp<sup>2</sup>C-H groups, in olefinic configurations (3000 cm<sup>-1</sup>) is also observed when increasing V<sub>b</sub>, while, on the contrary, the proportion of the sp<sup>2</sup>C-H complexes in aromatic rings (3065 cm<sup>-1</sup> + 3125 cm<sup>-1</sup>) increases significantly at the same time, suggesting a relative increase in the C=C configurations in aromatic features.

The presence of these features for high V<sub>b</sub> values is also confirmed by the enlargement of the well-defined absorption band at low frequencies range (950 -750 cm<sup>-1</sup>) which contains vibrations of C-H bonds, located at 865 cm<sup>-1</sup>, corresponding to one atom per cycle, and at 825 cm<sup>-1</sup>, related to two or three H atoms per cycle, as evidenced by the IR spectra presented in Fig. 5, is in good agreement with previous results [7]. This figure also shows intense IR absorption band around 1100 cm<sup>-1</sup> characteristic of Si-O complexes, probably due to the native oxide contamination on the silicon substrates.

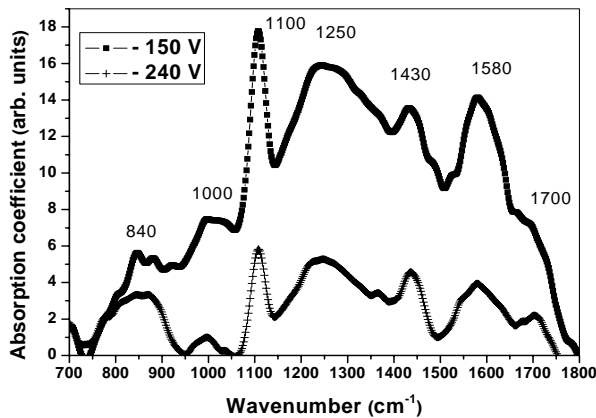


**Figure 5:** Typical FTIR spectra in the bending modes range for series I and IV.

The changes in the C-C bonding configurations are monitored by Raman spectroscopy measurements, after subtracting the photoluminescence background, in the 1000 – 1800 cm<sup>-1</sup> range. It is to be mentioned that Raman experiments probe in this range, essentially the sp<sup>2</sup>C atoms environment. Typical Raman spectra obtained for the four series of films are presented in Fig. 6. The Raman spectra exhibit a main well-defined peak centred at 1537-1550 cm<sup>-1</sup>, and a shoulder at lower wavenumber at 1333-1355 cm<sup>-1</sup>. By analogy with graphite [8], the main line is assigned to the 'G' peak, centred at 1580 cm<sup>-1</sup>, which is due to the bond stretching of all pairs of sp<sup>2</sup>C atoms. The less intense shoulder is related to the 'D' peak and is due to the breathing modes of sp<sup>2</sup> atoms in rings [1, 9].

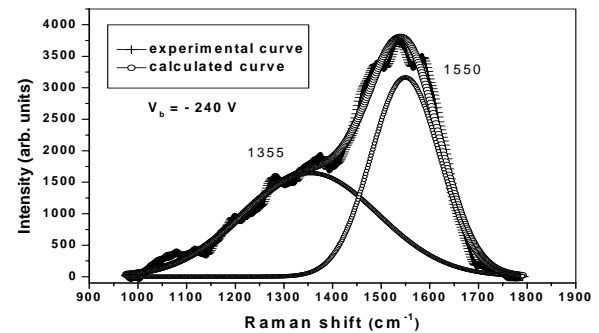
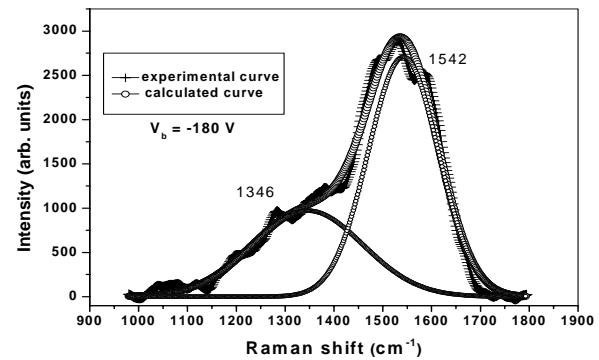
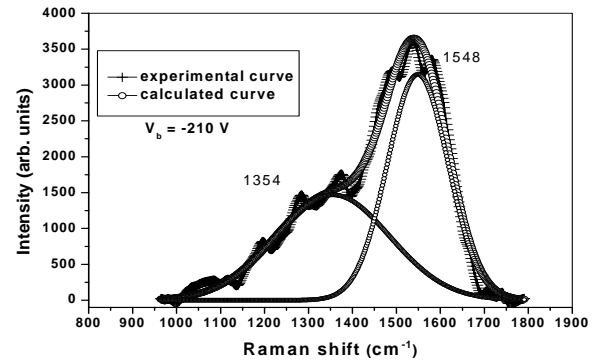
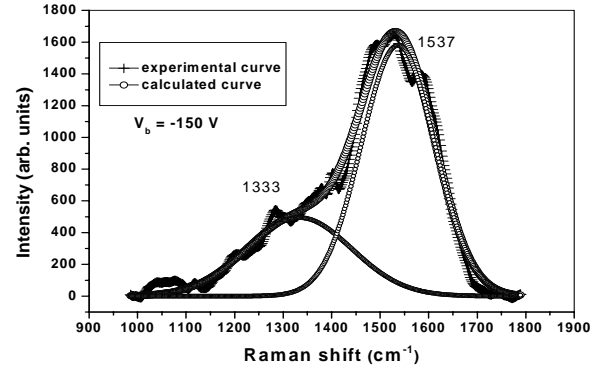


**Figure 6:** Decomposition of the Raman spectra of a-C:H films deposited at -150, -180, -210 and -240 V into a sum of two Gaussian contributions for different V<sub>b</sub> values. The fitted curves are also shown.

The 'D' peak is related to disorder and appears in microcrystalline and defective graphite. The decomposition of the Raman spectra into two Gaussian contributions (see Fig. 6) along these lines shows that both 'G' and 'D' peaks shift towards high wavenumbers with increasing  $V_b$ . The 'G' peak becomes narrower with increasing  $V_b$  while the FWHM of 'D' peak increases. On the other hand, both intensities of 'G' and 'D' peaks increase with increasing  $V_b$ . We summarize in Table 1 all the fitting parameters obtained from the decomposition of the Raman spectra of Fig. 6. The shift of the 'D' peak to higher frequencies with increasing  $V_b$  indicates a relative reduction of  $sp^3C$  sites. Indeed, the desorption of hydrogen under ionic bombardment promotes the formation of  $sp^2C$  sites and the graphitization of the material. These results are in good agreement with infrared data (see Fig. 3 and Fig. 4). Theye et al. [7] have assigned the wide 'D' band to collective vibrations of the continuously connected carbon 'skeleton' formed by both the  $sp^3$  and the  $sp^2$  C atoms. The sixfold ring breathing mode of  $A_{1g}$  symmetry, which is forbidden in graphite but becomes active in the presence of disorder, could also contribute to this band, particularly at high  $V_b$  [7]. This assumption is in agreement with the presence of aromatic rings as shown by the analysis of infrared absorption data of Fig. 4. Additional information about C-C bonding can be obtained from low frequency range of the infrared absorption spectra. In all samples, we can observe a well-visible band around  $1600\text{ cm}^{-1}$  which is attributed to the stretching modes of the C=C double bonds in different configurations [10]. The slight shift of this peak to lower wavenumbers and its enlargement as  $V_b$  increases (Fig. 5) is consistent with the formation of ring-like clusters instead of chain-like ones [10]. Beeman et al. [11] found that the G band position shifts to higher wavenumbers with increasing  $sp^2$  aromatic sites. According to this, as shown in Table 2, the G peak position shifts to higher frequencies indicating graphitization of the samples, when  $V_b$  increases.

$V_b$ (-V)	'G' peak			'D' peak			ID/IG
	Position ( $\text{cm}^{-1}$ )	Intensity	$\Delta G$ ( $\text{cm}^{-1}$ )	Position ( $\text{cm}^{-1}$ )	Intensity	$\Delta D$ ( $\text{cm}^{-1}$ )	
150	1537	1580	178	1333	494	253	0.44
180	1542	2707	169	1346	971	265	0.56
210	1548	3145	167	1354	1469	306	0.87
240	1550	3163	166	1355	1645	326	$\sim 1$

Table 2: Values of the different fitting parameters of the Raman spectra of Fig. 6. The values of the FWHM for the G ( $\square G$ ) and D ( $\square D$ ) peaks are also given in this Table.

The graphitization of the structure due to the loss of hydrogen can be followed by the evolution of the ratio of the integrated intensity of the D peak over that of the G one, ID/IG. As shown in Table 1, this ratio increases with the bias voltage  $V_b$  and therefore we can conclude, according to Ferrari and Robertson [1], that our films become more graphitic and contain more ordered rings rather than olefinic chains. The ID/IG ratio increases from

0.44 to  $\sim 1$  for  $V_b$  increasing from  $-150$  to  $-240$  V, as it is indicated in Fig. 7.

$V_b$ (-V)	150	180	210	240
$E_T$ (eV)	1.45	1.43	1.34	1.32
$E_{04}$ (eV)	1.93	1.83	1.75	1.74
$E_{04} - E_{Tauc}$ (eV)	+0.48	+0.40	+0.41	+0.42

Table 3: Values of optical gaps  $E_T$  and  $E_{04}$  for different values of  $V_b$ , as indicated.

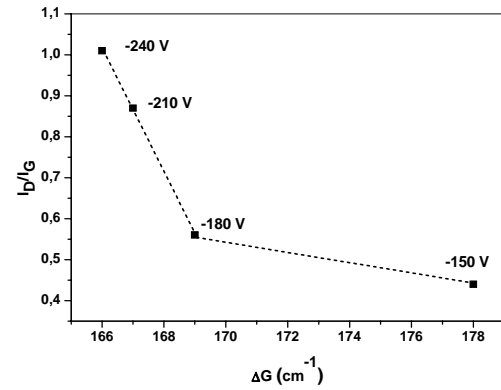


Figure 7: The ID/IG ratio plotted against the G peak FWHM for different values of  $V_b$ , as indicated.

Moreover, the optical gaps (Tauc's gap ( $E_T$ ) as well as  $E_{04}$ ) decrease with increasing  $V_b$ , as summarized in Table 3, suggesting an increase of the  $sp^2C$  sites at the expense of the  $sp^3C$  sites. Following the three-stages model of Robertson [1, 14], the decreasing of  $E_T$  and  $E_{04}$  with increasing  $V_b$ , suggest a slight increase of the aromatic clusters sizes when  $V_b$  increases. On the other hand, Schwan et al. [12] have proposed that the G peak width,  $\square G$ , is partially determined by the graphitic cluster size and a plot of ID/IG versus  $\square G$  should give a straight line. We summarize in Fig. 7 the variation of the ID/IG ratio as a function of  $\square G$ . It clearly shows that we do not observe a linear behaviour in the whole range of  $V_b$ . It seems that the variation of ID/IG as a function of  $\square G$  follows two different regimes, a first one between  $-150$  and  $-180$  V and the second one, linear, above  $-180$  V.

The second regime suggests that at relative high ion impact energies, the width of the G peak is affected by the presence of aromatic clusters, while for films deposited at  $-150$  V, the H content is relatively higher and the material contains more  $sp^3C$  atoms, so that the width  $\square G$  is not very influenced by the presence of graphitic clusters, as only a slight change is observed in the ID/IG ratio for  $V_b$  increasing from  $-150$  to  $-180$  V. One reason for this might be that the graphitic clusters now have H-terminated aromatic groups, rather than extended networks of graphene sheets. Another possibility, as it was previously suggested [13], is that the increased H

content might affect the elastic constants of the film and consequently affects the stress levels. Schwan et al. [12] have also proposed that a-C:H films with  $\square G$  greater than 45 cm<sup>-1</sup> have small aromatic clusters with size less than 10 Å. In our films, the very broad G peak width and the ID/IG ratio below one, suggest that aromatic clusters are less than 10 Å in size, and are thus probably composed of localised benzene-like or naphthalene-like structures. However, Ferrari and Robertson [1] showed that the disorder due to distortions would be a parameter which limits the size of these graphitic clusters.

## CONCLUSION

We presented a detailed investigation of the microstructure of a-C:H films prepared by rf-PECVD by varying the self-bias voltage  $V_b$  between -150 and -240 V. We demonstrated that this parameter, which reflects the incident ion energy, can play a major role in the structural evolution of our films. Bias induces a loss of the hydrogen content and thus a graphitization of the material, whose structure is characterized by H bonding to sp<sup>3</sup>C sites, preferentially, as revealed by infrared transmission data. Raman spectroscopy was also used to probe the microstructure and showed that the increase of  $V_b$  is accompanied by an increase in the number of sp<sup>2</sup>C graphitic clusters with limited sizes. Moreover, all samples are characterized by low hydrogen content (as revealed by absorbance values), an ID/IG ratio less than one and typical values of band gaps. These trends suggest that the structure of our a-C:H films which is composed of sp<sup>2</sup> aromatic sites embedded in a sp<sup>3</sup> matrix, have properties lying between those of polymeric a-C:H and Diamond-Like films.

**Acknowledgements** The authors are deeply indebted to M. Ouchabane and T. Kerdja from CDTA (Algiers) for the preparation of the a-C:H samples, and to C. Godet from PALMS Laboratory, University of Rennes (France) for helpful discussions.

## REFERENCES

- [1] A.C. Ferrari, and J. Robertson, "Interpretation of Raman spectra of disordered and amorphous carbon", *Phys. Rev. B* 61, (2000), pp. 14095 - 14106
- [2] R. Haerle, E. Riedo, A. Pasquarello, and A. Baldereschi, "sp<sup>2</sup>/sp<sup>3</sup> hybridization ratio in amorphous carbon from C 1s core-level shifts: X-ray photoelectron spectroscopy and first-principle calculation", *Phys. Rev. B* 65, (2001), pp. 045101 - 045109
- [3] B. Bushan, "Chemical, mechanical and tribological characterization of ultra-thin and hard amorphous carbon coatings as thin as 3.5 nm: recent developments", *Diamond Relat. Mater.* 8, (1999), pp. 1985 - 2015
- [4] C. Casiraghi, F. Piazza, A.C. Ferrari, D. Grambole, and J. Robertson, "Bonding in hydrogenated diamond-like carbon by Raman spectroscopy", *Diamond Relat. Mater.* 14, (2005), pp. 1098 - 1102
- [5] N.A. Morrison, S.E. Rodil, A.C. Ferrari, J. Robertson, and W.I. Milne, "High rate deposition of ta-C:H using an electron cyclotron wave resonance plasma source", *Thin Solid Films* 337, (1999), pp. 71 - 73
- [6] B. Racine, M. Benlahsen, K. Zellama, R. Bouzerar, J.P. Kleider, and H.J. von Bardeleben, "Electronic properties of hydrogenated amorphous carbon films deposited usin ECR-RF plasma method", *Diamond Relat. Mat.* 10, (2001), pp. 200 - 206
- [7] M.-L. Theye, V. Paret, and A. Sadki, "Relations between the deposition conditions, the microstructure and the defects in PECVD hydrogenated amorphous carbon films; influence of the electronic density of states", *Diamond Relat. Mat.* 10, (2001), pp. 182 - 190
- [8] M.A. Tamor, and W.C. Vassell, "Raman "fingerprinting" of amorphous carbon films", *J. Appl. Phys.* 76, (1994), pp. 3823 - 3830
- [9] S. Piscanec, M. Lazzeri, F. Mauri, A.C. Ferrari, and J. Robertson, "Kohn anomalies and electron - phonon interactions in graphite", *Phys. Rev. Lett.* 93, (2004), pp. 185503/1 - 185503/4
- [10] Y. Bounouh, K. Zellama, A. Zeinert, M. Benlahsen, M. Clin, and M.-L. Theye, "Modes of hydrogen incorporation in hydrogenated amorphous carbon (a-C:H); modifications with annealing temperature", *J. Phys. III France* 7, (1997), pp. 2159 - 2164
- [11] D. Beeman, J. Silverman, R. Lynds, and M.R. Anderson, "Modeling studies of amorphous carbon", *Phys. Rev. B* 30, (1984), pp. 870 - 875
- [12] J. Schwan, S. Ulrich, V. Batori, H. Errhardt, and S.R.P. Silva, "Raman spectroscopy on amorphous carbon", *J. Appl. Phys.* 80, (1996), pp. 440 - 447
- [13] J. Filik, P.W. May, S.R.J. Pearce, R.K. Wild, and K.R. Hallam, "XPS and laser Raman analysis of hydrogenated amorphous carbon films", *Diamond Relat. Mat.* 12, (2003), pp. 974 - 978
- [14] J. Robertson, "Diamond-like amorphous carbon", *Mater. Sci. Eng. R* 37, (2002), pp. 129 - 281